

Supporting Information

Visible Light Driven Mesoporous Ag-embedded ZnO Nanocomposite: Reactive Oxygen Species Enhanced Photocatalysis, Bacterial Inhibition and Photodynamic Therapy

Jagriti Gupta^a, Jeotikanta Mohapatra^b and D. Bahadur^{a*}

^aDepartment of Metallurgical Engineering and Materials Science

^bCentre for Research in Nanotechnology and Science (CRNTS)
Indian Institute of Technology Bombay, Mumbai – 400076, India

*Corresponding author. Tel.: +91 22 2576 7632; Fax: +91 22 2572 3480.

E-mail address: dhiren@iitb.ac.in

(a) Characterization techniques: X-ray diffraction (XRD) patterns were recorded on a PANalytical's X'Pert PRO diffractometer with Cu K α radiation. The crystallite sizes were estimated using Scherrer's calculator of X'Pert High Score Plus software. The transmission electron micrographs (TEM) were recorded by JEOL JEM-2100F HR-TEM and scanning electron micrographs (SEM) and elemental analyses of samples were carried out by JEOL JSM-7600F FEG-SEM. UV-visible spectra were recorded with a UV-visible spectrophotometer (Cecil, Model No. CE3021). The photoluminescence (PL) spectra of ZnO and Ag-ZnO NCs were recorded at room temperature using the excitation with a He-Cd laser ($\lambda = 325$ nm). XPS analysis was performed on a Multilab 2000 (Thermo VG Scientific) using Al K α ($h\nu = 1486.6$ eV) as the exciting source for identification of the elements and chemical status with the electronic database. The binding energies obtained in the XPS analysis of samples were standardized for specimen charging using C (1s) as the reference at 285 eV. The surface area and porosity measurements were performed by a Micromeritics ASAP 2020 surface area and porosity analyzer. During the measurement, samples were degassed at 90 °C for 2 h and then at 150 °C for 4 h.

(b) XPS spectra of Ag₅-ZnO NCs: XPS has been performed to investigate the chemical state of Ag and Zn in Ag₅-ZnO NCs. Fig. S1 shows the XPS spectra of (a) Zn 2p, (b) O 1s of Ag₅-ZnO NCs, and (c and d) Ag 3d. Two adjacent peaks at 368.2 eV and 374.1 eV are observed for Ag 3d corresponding to Ag 3d_{5/2} and Ag 3d_{3/2}, respectively, indicating a metallic nature of silver [1]. XPS spectra of Ag in Ag₁-ZnO NCs show two sharp peaks at 367.5 and 373.5 eV (Fig. S1d). The former could be fitted to two components; a major one at 367.5 eV with a very minor one at 368.2 eV. This suggests that most silver goes as Ag⁺ ions and occupy Zn site (Ag_{Zn}) and only a few Ag nanoparticle forms and presumably goes into interstitials. Further no peak corresponding to Ag₂O (367.8 eV) or AgO (367.4 eV) is observed in the Ag 3d spectra of Ag₅-ZnO NCs, indicating that the Ag embedded on ZnO NAs are in form of metallic Ag. The Zn2p spectrum shows peaks at 1022.6 and 1045.8 eV that correspond to the 2p_{3/2} and 2p_{1/2} lines for Zn²⁺ in ZnO. The deconvoluted O 1s spectrum shows three peaks positioned at 531.6 534 and 535.3 eV corresponding to the oxygen species present in the lattice (hydroxyl groups, oxygen vacancies or defects, surface absorbed oxygen species and surface hydroxyl groups) [2, 3]. These intense surface absorbed oxygen species in Ag-ZnO NCs help to trap the photoinduced electrons and enhance the photocatalytic performance.

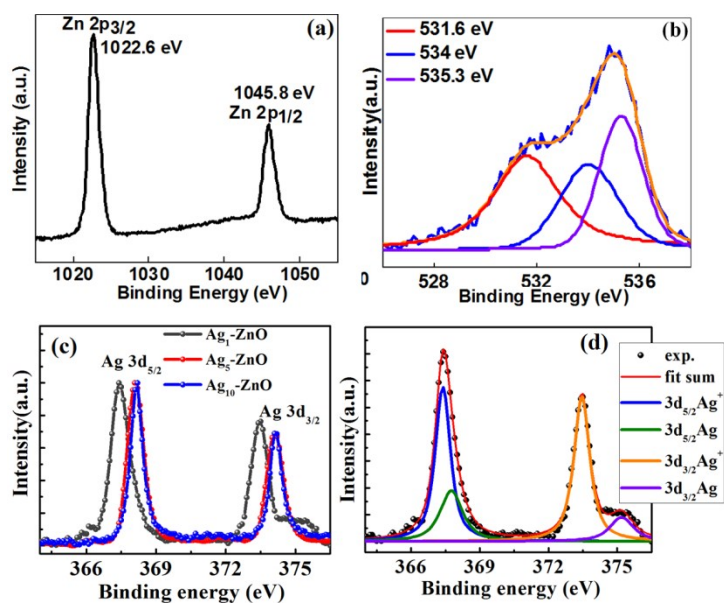


Fig. S1. High-resolution XPS spectra of: (a) Zn2p, (b) O 1s of Ag₅-ZnO NCs. (c) Ag-ZnO NCs and, (d) deconvolution of Ag (3d) of Ag₁-ZnO NCs

(c) SEM images and elemental analysis of Ag-ZnO NCs

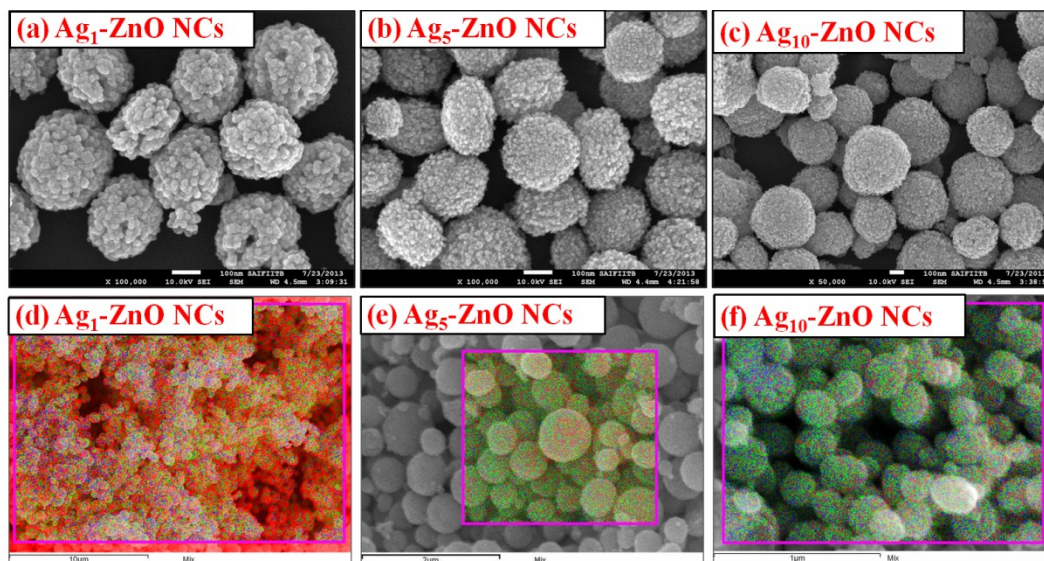


Fig. S2. SEM micrographs of (a) Ag₁-ZnO, (b) Ag₅-ZnO and (c) Ag₁₀-ZnO NCs. SEM-EDS spectral mapping of Ag in (d) Ag₁-ZnO, (e) Ag₅-ZnO, and (f) Ag₁₀-ZnO NCs, which shows the presence of Ag in the respective Ag-ZnO NCs, and their distribution (green points; Zn²⁺, red points; O, blue points: Ag).

Table S1. Elemental compositions of Ag-ZnO NCs measured by EDS

Sample Name	Conc. of Zn and Ag (wt %)by EDS analysis	
	Zn	Ag
Ag ₁ -ZnO	79.3	0.8
Ag ₅ -ZnO	73.7	2.8
Ag ₁₀ -ZnO	70.8	5.9

(d) Surface area and porosity analysis of Ag-ZnO NCs

The N₂ gas adsorption-desorption isotherms display the typical type IV curve following a type H₃ hysteresis loop which is usually attributed to the predominance of mesopores. The BET surface areas of the ZnO and Ag-ZnO NCs are given in the Table S2.

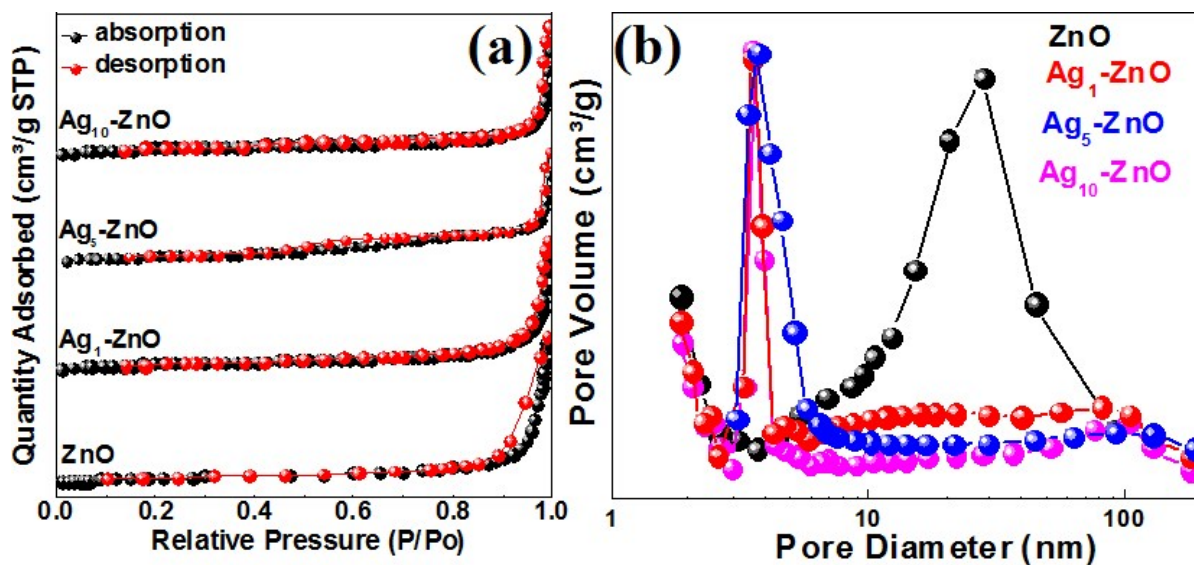


Fig. S3. (a) Absorption-desorption curve and (b) the pore size distribution of ZnO, Ag₁-ZnO, Ag₅-ZnO and Ag₁₀-ZnO NCs.

Table S2. The surface area, pore size, and pore volume of Ag-ZnO NCs.

Sample Name	BET Surface area (m ² /g)	Pore volume (cm ³ /g)	Pore Diameter (nm)
ZnO	23.4	0.19	28
Ag ₁ -ZnO	32.2	0.18	53
Ag ₅ -ZnO	25.6	0.15	15
Ag ₁₀ -ZnO	39.3	0.19	27

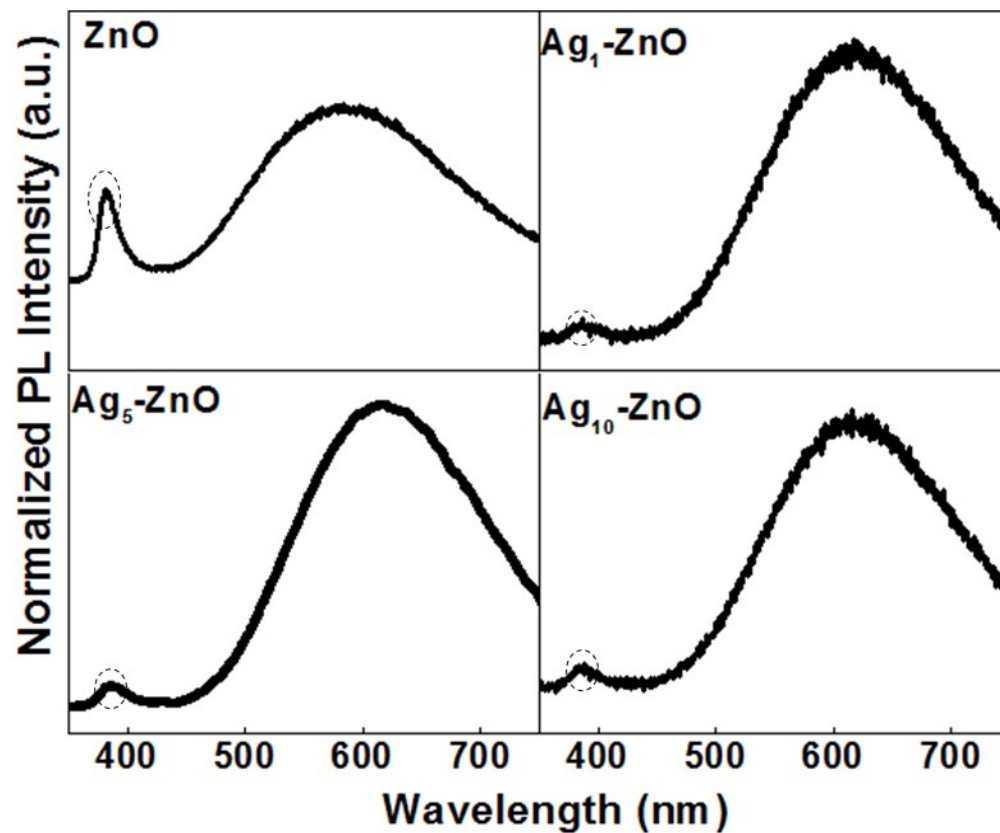


Fig. S4. PL spectra of ZnO and Ag-ZnO NCs. The dotted circle shows the decrease in intensity of UV band emission.

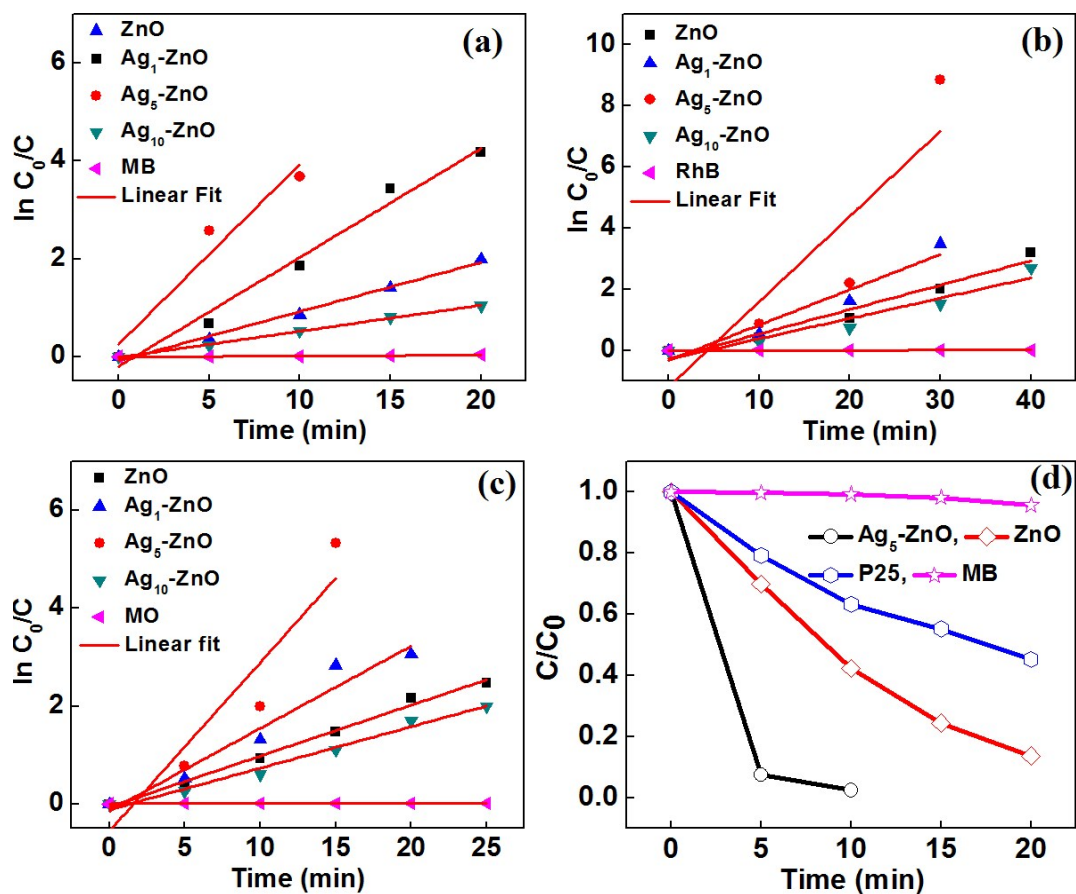


Fig. S5. Kinetics of photocatalytic degradation of (a) MB, (b) RhB, and (c) MO using ZnO, Ag-ZnO NCs as photocatalysts, and (d) Photocatalytic degradation of MB using ZnO, P25 and Ag₅-ZnO NCs under solar light for a comparative performance

Table S3. Photocatalytic performance of Ag-ZnO NCs

Structural Morphology	Dyes/conc.	Catalyst conc/ reaction Vol.	light Source/efficiency with time	Referenc e
Ag-ZnO nanofibers	RhB 2.5×10 ⁻⁵ M	10mg 10 ml	8 W, UV light 100 %, 50 min	4
Ag-ZnO nanocomposite	MO, MB, 4-NP 10 ppm	2mg 20 ml	400 W, visible light 100 % MO; 5, MB; 4, 4-NP; 6h	5
Ag nanoparticles loaded ZnO nanoflakes	MO 0.03mM	25mg 25ml	300 W, Xe lamp UV light 76 % 60 min	6
Ag@ZnO nanocomposites	MB 10ppm	2mg 20 ml	400 W, visible light 97.43%, 5h	7
porous 3D flower-like Ag/ZnO (AZ-15)	RhB	0.04 g 20 ml	175 W (Hg UV lamp) 500 W (Xenon lamp) 79%, 120 min	8
Ag@ZnO on Cotton Fabrics	RhB 0.01 mM	5 mg 3 ml	400 W (visible light) 100 %, 1.5 h	9
Ag/ZnO NRs, NWs	RhB	2mg/ml 3 ml	9W, visible light 82%, 4h	10
Hierarchical nanostructured Ag-ZnO	MB 10 ppm	10 mg 3 ml	Direct Solar light between (11 am -1 pm) 97 %, 60 min	11
Ag-ZnO NCs	MB, RhB, MO	50 mg 100 ml	Solar light (Xe lamp (350 W) 100 %,MB; 10, RhB ; 30, MO; 15 min	present work

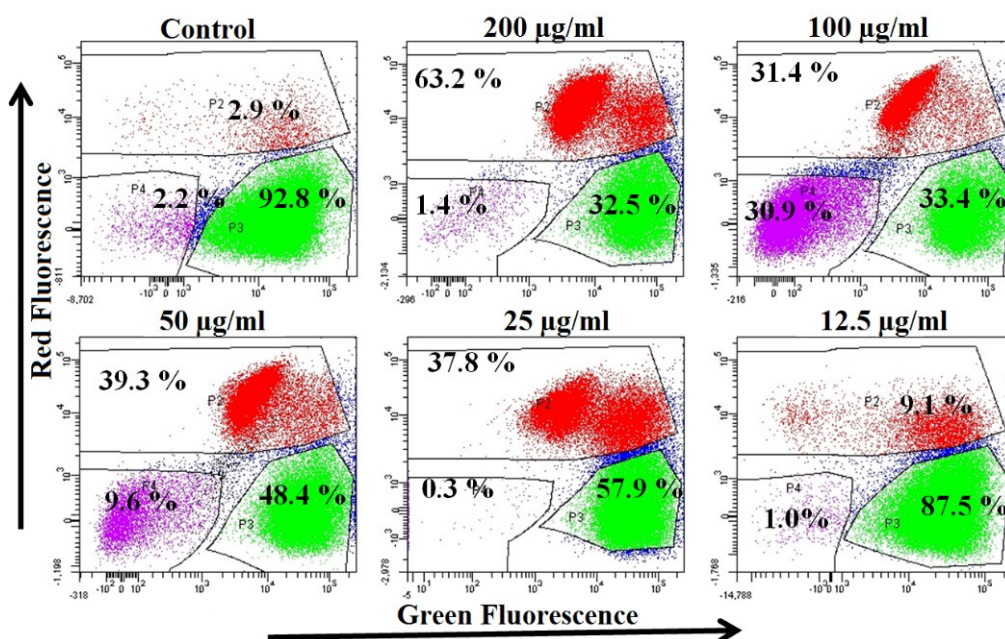


Fig. S6. Flow cytometric analysis of *E. coli* Control, treated with 200 to 12.5 $\mu\text{g/ml}$ $\text{Ag}_5\text{-ZnO}$ NCs for 2 h, stained with SYTO9 and PI.

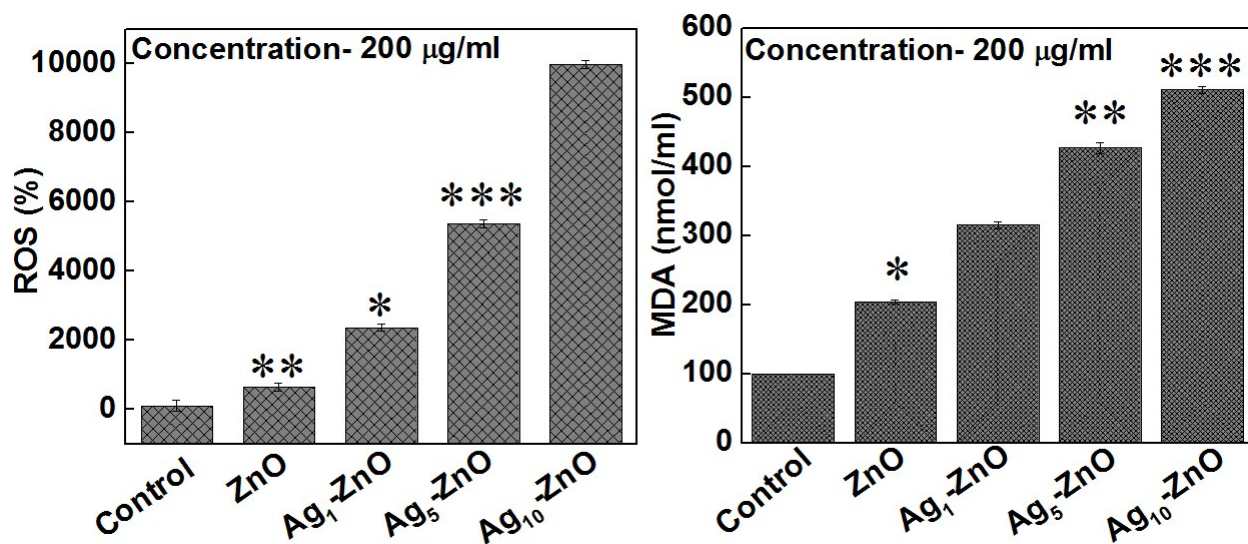


Fig. S7. (a) Generation of ROS, and (b) MDA equivalent in *E. coli* after 2 h treatment with $200 \mu\text{g/ml}$ of ZnO, $\text{Ag}_1\text{-ZnO}$, $\text{Ag}_5\text{-ZnO}$, and $\text{Ag}_{10}\text{-ZnO}$ NCs.

(e) Bacterial membrane potential of *E. coli*: The cell membrane disruption and membrane potential of *E. coli* has been analyzed by the FACS using 3, 3'-diethyloxa-carbocyanine iodide dye (DiOC_2). Fig. S8 shows the membrane potential of *E. coli* on treatment with ($200 \mu\text{g/ml}$)

Ag₅-ZnO- NCs for 2 h. DiOC₂ exhibits green fluorescence, but the fluorescence shifts toward red emission as the dye molecules self-associate at the higher cytosolic concentrations caused by high membrane potential. Fig. S8a shows the change in the membrane potential of the control *E. coli* without any treatment and Figure S8b shows the change in the membrane potential on treatment with 200 µg/ml of Ag₅-ZnO NCs. Depolarization of bacterial cell membranes has been observed as a shift of DiOC₂ fluorescence from green to red. This shift is higher in Ag₅-ZnO NCs with respect to control. The increase in red fluorescence and decrease in green fluorescence confirm that Ag₅-ZnO NCs significantly damage the membrane integrity of *E. coli*.

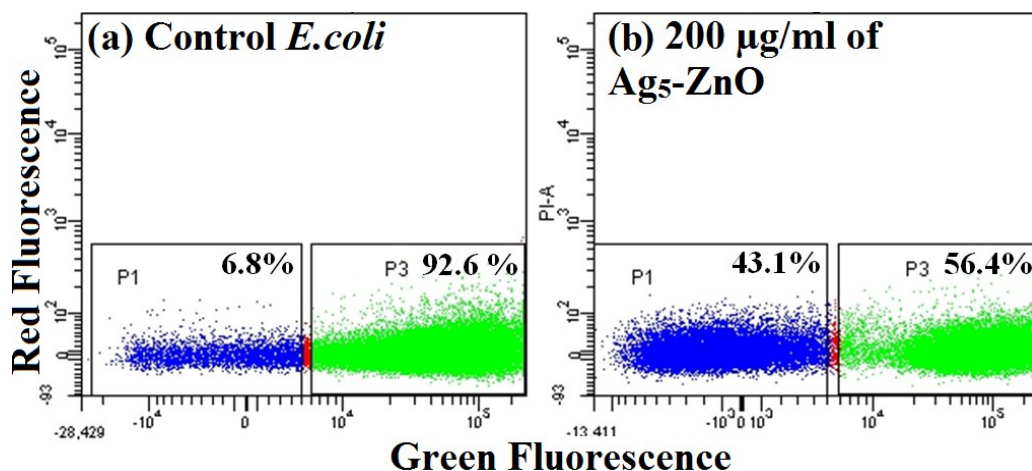


Fig. S8. Flow cytogram depicting the changes in (a) membrane potential of *E. coli* treated with 0, 200 µg/ml of Ag₅-ZnO NCs for 2 h. In the flow cytogram, P1 region (blue) indicate cells with polarized bacterial membrane potential while P3 scatter region (green dots) denotes cells with depolarized membrane potential of *E. coli*.

(f) Change in mitochondrial membrane potential (MMP) and morphologies of KB cells after treatment with Ag₅-ZnO NCs

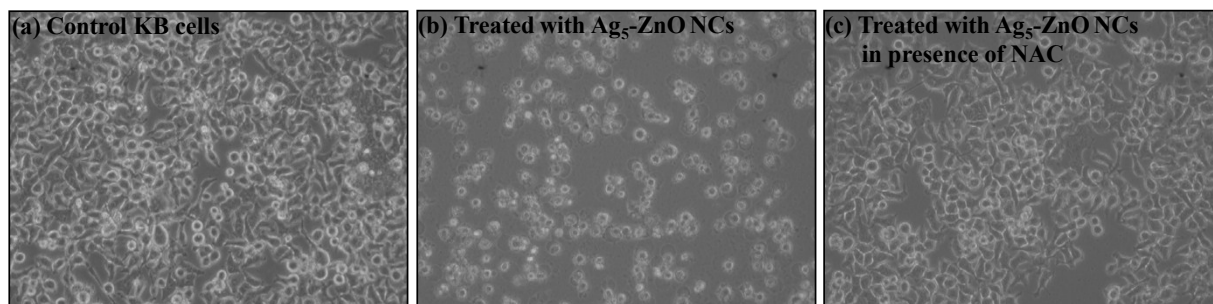


Fig. S9. Optical microscopic images of (a) control KB cells, and (b) KB cells treated with 50 µg/ml of Ag₅-ZnO NCs under light for 1 h exposure, and (c) KB cells treated with 50 µg/ml of Ag₅-ZnO NCs under light for 1 h exposure in presence of N-acetyl cysteine. Image was taken at 10X.

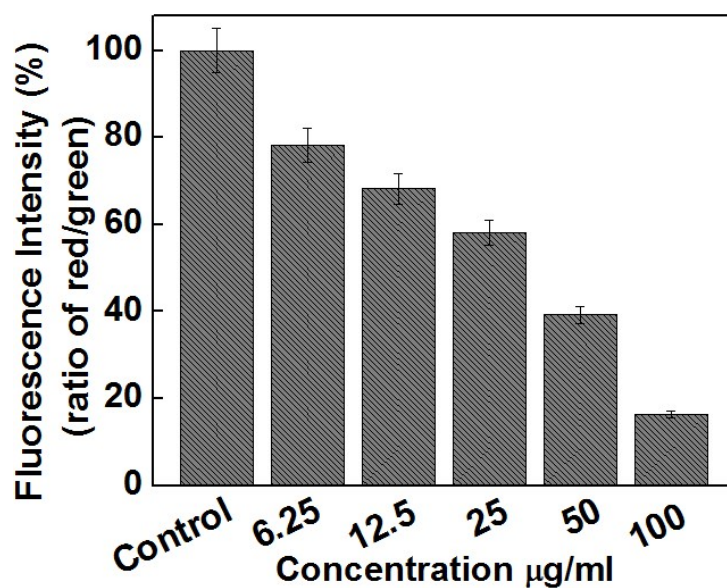


Fig. S10. Mitochondrial membrane potential of KB cells after treatment with Ag₅-ZnO NCs after 1h visible light irradiation.

References

- [1] Y. Zhang, S. Guo, J. Ma and H. Ge, *J. Sol-Gel Sci. Technol.*, 2014, 72, 171-178.
- [2] P. V. AshaRani, G. Low Kah Mun, M. P. Hande and S. Valiyaveetil, *ACS Nano*, 2008, 3, 279-290.
- [3] X. Xu, D. Chen, Z. Yi, M. Jiang, L. Wang, Z. Zhou, X. Fan, Y. Wang and D. Hui, *Langmuir*, 2013, 29, 5573-5580.
- [4] D. Lin, H. Wu, R. Zhang and W. Pan, *Chem. Mater.*, 2009, 21, 3479-3484.
- [5] S. A. Ansari, M. M. Khan, M. O. Ansari, J. Lee and M. H. Cho, *J. Phys. Chem. C*, 2013, 117, 27023-27030.
- [6] W. L. Ong, S. Natarajan, B. Kloostra and G. W. Ho, *Nanoscale*, 2013, 5, 5568-5575.
- [7] S. A. Ansari, M. M. Khan, J. Lee and M. H. Cho, *J. Ind. Eng. Chem.*, 2014, 20, 1602-1607.
- [8] Y. Liang, N. Guo, L. Li, R. Li, G. Ji and S. Gan, *Appl. Surf. Sci.*, 2015, 332, 32-39.
- [9] J. Manna, S. Goswami, N. Shilpa, N. Sahu and R. K. Rana, *ACS Applied Mater. Interfaces*, 2015, 7, 8076-8082.
- [10] Y. Liu, S. Wei and W. Gao, *J. Hazard. Mater.*, 2015, 287, 59-68.
- [11] S. S. Patil, M. G. Mali, M. S. Tamboli, D. R. Patil, M. V. Kulkarni, H. Yoon, H. Kim, S. S. Al-Deyab, S. S. Yoon, S. S. Kolekar and B. B. Kale, *Catal. Today*, 2016, 260, 126-134.